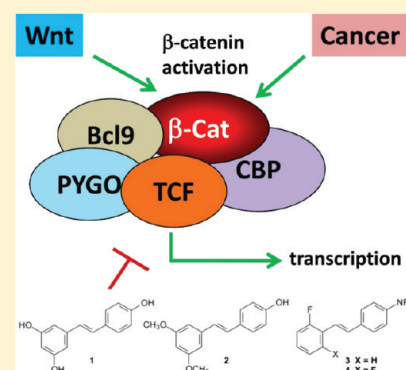


# Fluorinated *N,N*-Dialkylaminostilbenes for Wnt Pathway Inhibition and Colon Cancer Repression

Wen Zhang,<sup>†,§</sup> Vitaliy Sviripa,<sup>†</sup> Liliia M. Kril,<sup>†</sup> Xi Chen,<sup>†,§</sup> Tianxin Yu,<sup>†,§</sup> Jiandang Shi,<sup>†,§</sup> Piotr Rychahou,<sup>†,§</sup> B. Mark Evers,<sup>†,§</sup> David S. Watt,<sup>†</sup> and Chunming Liu<sup>\*,†,§</sup><sup>†</sup>Department of Molecular and Cellular Biochemistry, <sup>‡</sup>Department of Surgery, and <sup>§</sup>Markey Cancer Center, University of Kentucky, Lexington, Kentucky 40506-0509, United States**S** Supporting Information

**ABSTRACT:** Colorectal cancer (CRC) is the second leading cause of cancer-related mortality in the United States. CRC is initiated by mutations of the tumor suppressor gene, adenomatous polyposis coli (APC), or  $\beta$ -catenin gene. These mutations stabilize  $\beta$ -catenin and constitutively activate Wnt/ $\beta$ -catenin target genes, such as c-Myc and cyclin D1, ultimately leading to cancer. Naturally occurring stilbene derivatives, resveratrol and pterostilbene, inhibit Wnt signaling and repress CRC cell proliferation but are ineffective at concentrations less than 10  $\mu$ M. To understand the structure–activity relationship within these stilbene derivatives and to develop more efficacious Wnt inhibitors than these natural products, we synthesized and evaluated a panel of fluorinated *N,N*-dialkylaminostilbenes. Among this panel, (*E*)-4-(2,6-difluorostyryl)-*N,N*-dimethylaniline (**4r**) inhibits Wnt signaling at nanomolar levels and inhibits the growth of human CRC cell xenografts in athymic nude mice at a dosage of 20 mg/kg. These fluorinated *N,N*-dialkylaminostilbenes appear to inhibit Wnt signaling downstream of  $\beta$ -catenin, probably at the transcriptional level.



## INTRODUCTION

Wnt/ $\beta$ -catenin signaling plays an important role in development and tumorigenesis,<sup>1,2</sup> and the deregulation of Wnt signaling results in the formation of tumors. More than 90% of CRCs contain a mutation in APC or  $\beta$ -catenin,<sup>3–5</sup> and these mutations stabilize  $\beta$ -catenin and activate Wnt signaling. Cells containing these mutations constitutively activate Wnt signaling and undergo strong proliferation that ultimately leads to cancer.<sup>3</sup> Intercepting and blocking the Wnt pathway at various points in the signaling cascade is an attractive approach for CRC chemoprevention and therapeutics.

In normal cells,  $\beta$ -catenin degradation is under the control of Wnt signaling. In the absence of Wnt stimulation, the Axin complex, consisting of GSK-3, CK1 $\alpha$ , and the tumor suppressor proteins Axin and APC, phosphorylates  $\beta$ -catenin. Recognition of the phosphorylated  $\beta$ -catenin by the ubiquitin ligase  $\beta$ -Trcp triggers degradation by the ubiquitin/proteasome pathway.<sup>6,7</sup> Without  $\beta$ -catenin, the TCF/LEF family of transcription factors recruits the co-repressors Groucho and CtBP, repressing the expression of Wnt target genes.<sup>1</sup> When Wnt protein binds its receptor Frizzled and co-receptor LRP5/6, Wnt stimulates LRP5/6 phosphorylation in part through the recruitment of the cytoplasmic protein Disheveled.<sup>8</sup> Phosphorylated LRP5/6 then recruits Axin to the cell membrane, disrupts the Axin complex, and thus stabilizes  $\beta$ -catenin.<sup>8,9</sup> Accumulated  $\beta$ -catenin subsequently enters the nucleus, binds TCF/LEF, and recruits

transcriptional coactivators such as Bcl9, Pygopus, and CBP/p300 in order to activate downstream target genes, such as cyclin D1, c-Myc, survivin, and Axin2.<sup>1,3</sup>

In CRCs,  $\beta$ -catenin is stabilized by mutations of APC or  $\beta$ -catenin. APC truncations inhibit  $\beta$ -catenin phosphorylation, ubiquitination, and degradation.<sup>4,5,10</sup>  $\beta$ -Catenin mutations at N-terminal serine/threonine residues prevent  $\beta$ -catenin phosphorylation and thus prevent its ubiquitination and degradation.<sup>7</sup> These mutations decouple the regulation of  $\beta$ -catenin levels from upstream signaling events, and upstream inhibitors cannot efficiently inhibit Wnt signaling in CRCs. Thus, useful agents for CRC prevention and treatment must block the function of  $\beta$ -catenin in the nucleus through one of several mechanisms including blockade of nuclear translocation of  $\beta$ -catenin, assembly of the transcription complex, and/or promoter-specific histone modification.

Recently, several Wnt inhibitors were identified in high-throughput screening<sup>11,12</sup> that target the upstream signaling of  $\beta$ -catenin in order to promote  $\beta$ -catenin degradation. Although these agents efficiently inhibit Wnt signaling in normal cells and some APC-mutated CRC cells, they may not be effective in CRC cells containing  $\beta$ -catenin mutations.<sup>13</sup> Several other Wnt inhibitors have also been reported; however, side effects limit their

Received: September 27, 2010

Published: February 03, 2011

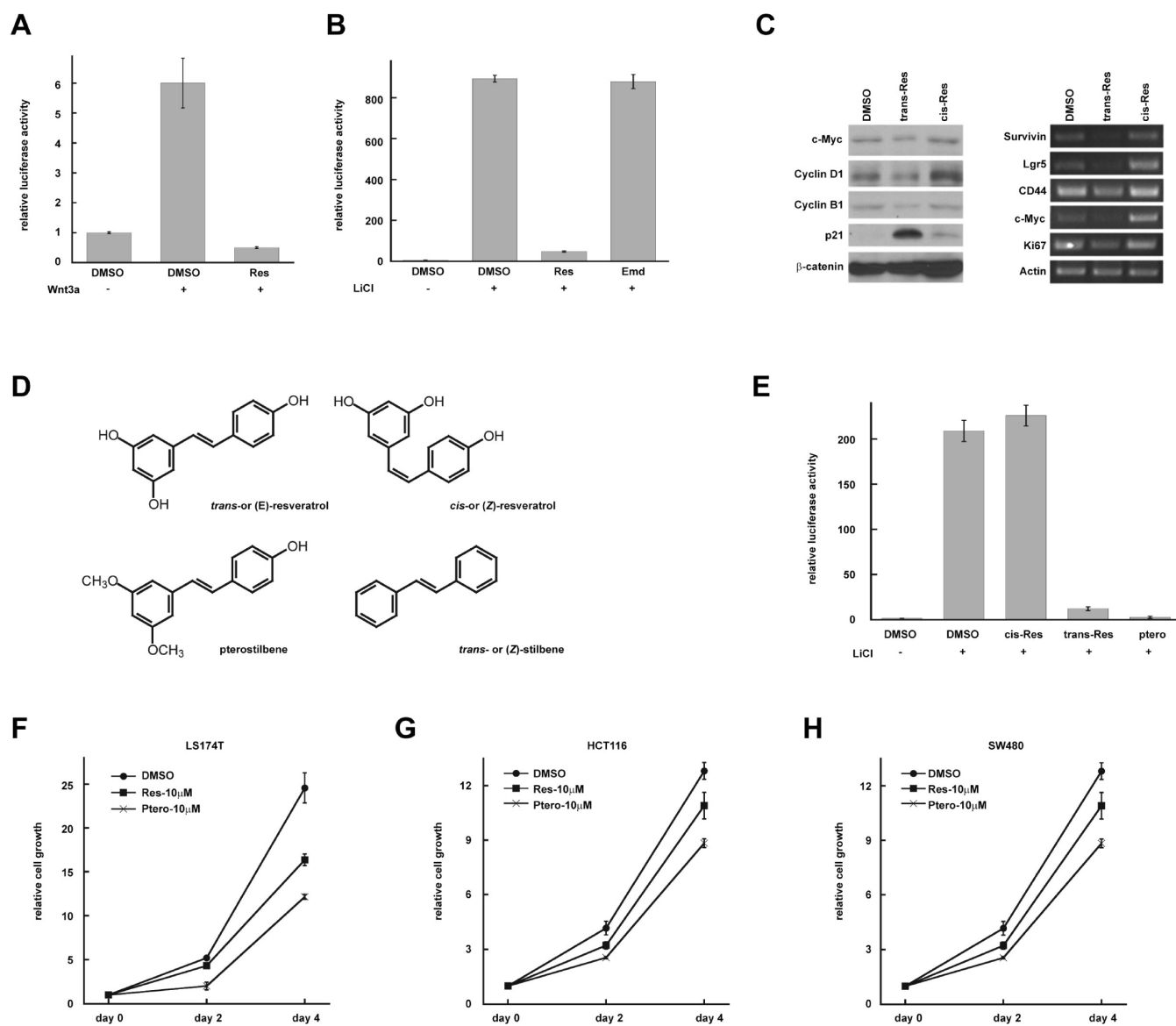


**Figure 1.** Resveratrol and pterostilbene inhibit Wnt signaling and repress proliferation of CRC cells. (A) Resveratrol (100  $\mu$ M) inhibits Wnt-induced TopFlash reporter activity. (B) Resveratrol (100  $\mu$ M) inhibits LiCl-induced TopFlash reporter activity. (C) Resveratrol (100  $\mu$ M) inhibits the expression of endogenous Wnt targets in CRC cells. Left panel shows protein levels. Right panel shows mRNA levels. (D) Structures of *trans*-resveratrol, *cis*-resveratrol, pterostilbene, and stilbene. (E) *trans*-Resveratrol and pterostilbene but not *cis*-resveratrol inhibits Wnt signaling at 100  $\mu$ M. (F–H) Resveratrol and pterostilbene inhibit the proliferation of CRC cell lines LS174, HCT116, and SW480.

potential utility in humans.<sup>14,15</sup> Natural products found in foods are potentially ideal chemopreventive and therapeutic agents for CRCs if they possess sufficient potency and minimal toxicity, and at the very least, natural products are a time-honored starting point for the synthesis of new pharmaceutical agents.

Resveratrol (*trans*-resveratrol or (*E*)-3,5,4'-trihydroxystilbene) is a phytoalexin produced in plants and popularized as a beneficial ingredient in red wine.<sup>16</sup> Resveratrol and other stilbene derivatives, including pterostilbene, a resveratrol analogue found in blueberries, exhibit anticancer activity.<sup>17,18</sup> Several studies have indicated that 10–100  $\mu$ M resveratrol inhibit Wnt signaling,<sup>19–21</sup> which suggests that inhibition of Wnt signaling may be important in mediating the chemopreventive function of these naturally occurring stilbenes. In this study, we designed and synthesized a panel of novel resveratrol analogues in order to identify more potent agents for Wnt pathway inhibition and CRC repression.

## RESULTS

**Natural Stilbene Analogues Resveratrol and Pterostilbene Inhibit Wnt Signaling.** To identify Wnt pathway inhibitors for CRC prevention and treatment, we screened a number of anticancer agents from plants using TopFlash reporter assay. The TopFlash reporter was transfected into HEK293T cells, and the cells were treated with Wnt3A-conditioned medium in order to activate the luciferase reporter (Figure 1A). Resveratrol (100  $\mu$ M) significantly inhibited Wnt-induced luciferase activity. To determine if resveratrol regulates  $\beta$ -catenin degradation, we treated the cells with 25 mM LiCl, which inhibits GSK-3 and stabilizes  $\beta$ -catenin. In this assay, LiCl activated the reporter more strongly than Wnt3A conditioned medium (Figure 1B). We found that resveratrol strongly inhibited LiCl-induced Wnt signaling, suggesting that resveratrol inhibits Wnt signaling by

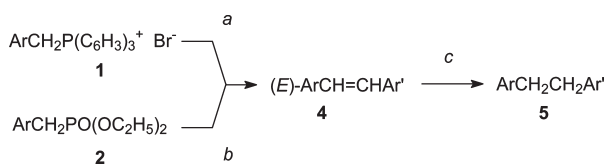


**Figure 2.** Synthesis of fluorinated *N,N*-dialkylaminostilbenes. Reagents: (a) (1) *n*-BuLi, THF; (2) ArCHO **3**; (b) (1) NaH, DMF; (2) ArCHO **3**; (c) H<sub>2</sub>, Pd–C, THF. Either Wittig or Wadsworth–Emmons reactions using phosphonium salts **1** or diethyl phosphonates **2**, respectively, with aldehydes **3** provided the *(E)*-stilbenes **4** in good yield. The phosphonium salts **1** were prepared from commercial samples of the corresponding benzyl bromides and triphenylphosphine, and the diethyl phosphonates **2** were prepared from the corresponding benzyl bromides and triethyl phosphite using the Arbuzov reaction according to standard literature procedures. The hydrogenation of **4n** using 10% Pd–C provided 4-(2,6-difluorophenethyl)-*N,N*-dimethylaniline (**5r**). Compounds were characterized fully, and purity (>95%) was established through combustion analyses.

regulating  $\beta$ -catenin activity but not its degradation. Emodin is an anticancer agent from plants;<sup>22</sup> it exists in many unpurified resveratrol products. We found that emodin had no effect on Wnt signaling (Figure 1B).

To confirm these results, we analyzed  $\beta$ -catenin target genes in LS174 CRC cells by Western blot and RT-PCR (Figure 1C). We found that the protein levels of c-Myc and cyclin D1, which are  $\beta$ -catenin targets, are reduced by resveratrol but not its isomer, *cis*- or (*Z*)-resveratrol (Figure 1C). Cyclin B1 levels were decreased, whereas p21<sup>WAF1/CIP1</sup> levels increased, consistent with the fact that p21<sup>WAF1/CIP1</sup> expression is repressed by c-Myc.  $\beta$ -Catenin levels were not affected by resveratrol. Next, we analyzed the mRNA levels of  $\beta$ -catenin target genes using RT-PCR. Expression of survivin, Lgr5, CD44, and c-Myc was decreased in resveratrol-treated cells. The cell proliferation marker, Ki67, also decreased. These results confirmed that resveratrol inhibits endogenous Wnt target genes in CRC cells.

Many stilbene derivatives also exhibit anticancer activity. To understand the structure–activity relationship of these compounds, we tested several resveratrol analogues (Figure 1D). We found that pterostilbene also inhibits Wnt signaling (Figure 1E). To study the effects of resveratrol and pterostilbene on cell growth, we treated LS174 CRC cells with resveratrol and pterostilbene for 2 and 4 days. We found that both compounds inhibited cell proliferation (Figure 1F). Similar results were observed with other CRC lines (Figure 1G,H). Pterostilbene was more active than resveratrol in these assays, suggesting that it is possible to identify better resveratrol analogues for Wnt inhibition and CRC repression.

**Fluorinated *N,N*-Dialkylaminostilbenes Are Potent Wnt Inhibitors.** Using resveratrol and pterostilbene as lead structures, we designed and synthesized a panel of stilbene analogues (Figures 2, 3A, and 4A). We first explored various monosubstituted hydroxy-, alkoxy-, amino-, and *N,N*-dialkylaminostilbenes using Western blot assay (Figure 3B,C), and of these substituents, *(E)*-4-styryl-*N,N*-dimethylaniline (**4d**) at 30  $\mu$ M with an *N,N*-dimethylamino substituent strongly repressed Wnt target genes, Axin2 and c-Myc, in CRC cells (Figure 3C). However, the solubility of **4d** was poor and it was not effective below 10  $\mu$ M (data not shown). To improve its solubility and activity, we modified **4d** with 2'-fluoro **4e**, 3'-fluoro **4f**, and 4'-fluoro **4g** substituents (Figure 3D). Although both **4e** and **4f** had promising activity at 10  $\mu$ M, *(E)*-4-(2-fluorostyryl)-*N,N*-dimethylaniline (**4e**)

was the best among all of the monofluoro-substituted compounds. We next examined modifications of the *N,N*-dimethylamino group within **4e** and found that the *N,N*-diethylamino group in *(E)*-4-(2-fluorostyryl)-*N,N*-diethylaniline (**4h**) is also active at 10  $\mu$ M but not as potent as **4e**, and the *N,N*-diphenylamino group in **4i** was inactive (Figure 3E). These analogues had no effects on  $\beta$ -catenin levels, further indicating that they affect  $\beta$ -catenin activity but not stability. We compared the effects of **4e**, resveratrol, and pterostilbene on CRC cell growth and found that **4e** is a much better inhibitor in the cell proliferation assay (Figure 3F).

On the basis of the improved activity seen in **4e** relative to **4d**, we synthesized difluorinated *N,N*-dimethylaminostilbenes in which at least one of the fluorine substituents is in the 2'- or 3'-position (Figure 4A). We found that the compounds with a 2'-fluoro and another fluoro ortho or meta to the double bond (**4m**, **4o**, and **4r**) are more active than **4e** (Figure 4B). The *(E)*-4-(2,6-difluorostyryl)-*N,N*-dimethylaniline (**4r**) had the best activity. The *o*- and *m*-*N,N*-dimethylamino analogues of **4r** (i.e., **4p** and **4q**) are not as active as **4r**, indicating that the *p*-dimethylamino in **4r** is important for its activity (Figure 4C). On the basis of the structure of **4r**, we also made two trifluorinated dimethylaminostilbenes **4v** and **4w** in which two of the fluorine substituents are in the 2'- and 6'-positions (Figure 4D). Although **4v** and **4w** were active at 10  $\mu$ M, they showed no significant improvements over **4r**. When the stilbene carbon–carbon double bond in **4r** was reduced to a saturated single bond in the 1,2-diarylethane **5r**, the activity was lost, suggesting that the double bond was necessary for biological activity (Figure 4D). We treated LS174 CRC cells with different dosages of **4r** and found that **4r** significantly inhibited Wnt target genes at 2.5  $\mu$ M and is even active at 0.5  $\mu$ M (Figure 4E).

Fluorinated *N,N*-dialkylaminostilbenes inhibit CRC in vitro and in vivo. We analyzed the effects of these novel agents on CRC cells growth. Consistent with the Western blot results, stilbene **4r** was more potent than **4e** in cell proliferation assay; it inhibited LS174 cell proliferation at nanomolar concentrations (Figure 5A). To test the effects of **4r** on tumor growth in vivo, we injected LS174 cells subcutaneously into the flanks of athymic nude mice. The mice were randomized into two groups. One group of mice was treated with **4r** (20 (mg/kg)/day) dissolved in corn oil by intraperitoneal (ip) injection. The control mice were treated with same volume of corn oil (50  $\mu$ L) by ip injection. The mice were weighed and tumors measured twice weekly. The **4r** treated mice and control mice have no significant difference in body weight within 1 month (Figure 5B and Figure 5C), suggesting that **4r** has no significant toxic effect at this dosage. However, the growth of tumor xenografts was significantly inhibited by **4r** treatment (Figure 5D).

Fluorinated *N,N*-dialkylaminostilbenes inhibit Wnt signaling in the nucleus. The stilbene analogues and in particular *(E)*-4-(2,6-difluorostyryl)-*N,N*-diethylaniline (**4s**) (Figure 4A) exhibit strong fluorescence at 365 nm (Figures 6A), albeit **4s** is slightly less active than **4r** (Figure B). Nevertheless, **4s** lends itself well to a mechanistic study of the site of action of these compounds. We treated LS174 cells with 10  $\mu$ M **4s** for 2, 6, 12, and 24 h. The cells were fixed and analyzed by confocal fluorescence microscopy. We found that **4s** was localized throughout the nucleus and cytoplasm at 2 h. After 12 h, the nuclear levels of **4s** were decreased (Figure 6C). To study the effects of these compounds on  $\beta$ -catenin localization, we treated LS174 cells with 10  $\mu$ M **4r** for 24 h. The cells were fixed, and  $\beta$ -catenin localization

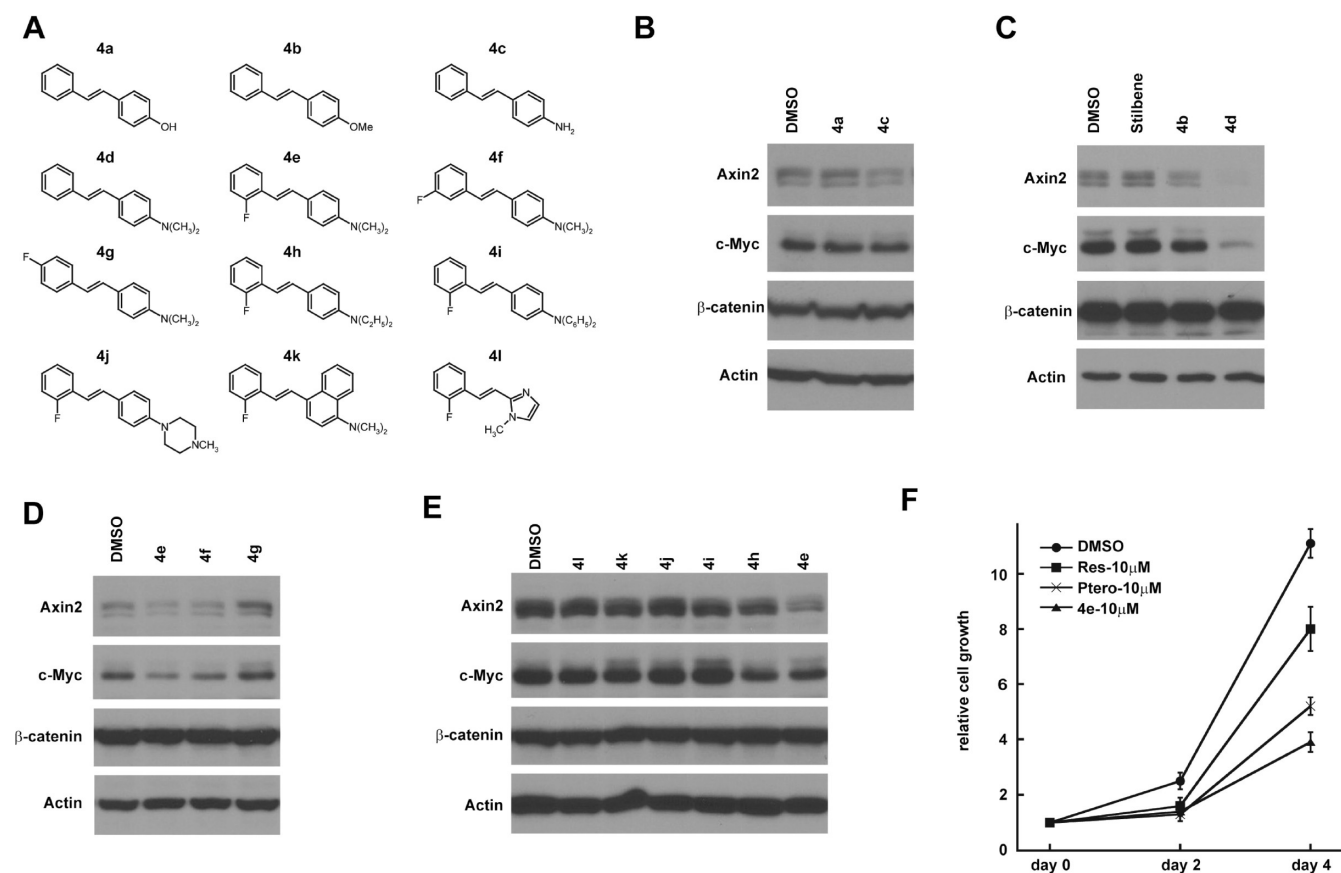


**Figure 3.** Fluorinated *N,N*-dialkylaminostilbenes inhibit Wnt signaling in CRC cells. (A) Chemical structure of synthesized resveratrol analogues. (B) 4-Aminostilbene (**4c**) represses Wnt target genes at 30  $\mu\text{M}$ . (C) 4-Styryl-*N,N*-dimethylaniline (**4d**) is more active than 4-methoxystilbene (**4b**) at 30  $\mu\text{M}$ . (D) 4-(2-Fluorostyryl)-*N,N*-dimethylaniline (**4e**) and 4-(3-fluorostyryl)-*N,N*-dimethylaniline (**4f**) repress Wnt target genes at 10  $\mu\text{M}$ . (E) The dimethylamino-phenyl group within **4e** is critical for its activity. (F) **4e** is more potent than resveratrol and pterostilbene in inhibiting the proliferation of CRC cells.

was analyzed by immunofluorescence (Figure 6D). The nuclear  $\beta$ -catenin levels were decreased in **4r** treated cells compared with the DMSO-treated cells. However, significant levels of nuclear  $\beta$ -catenin can still be detected in the nucleus of **4r** treated cells, suggesting that **4r** may also inhibit Wnt signaling through mechanisms other than regulation of  $\beta$ -catenin level and localization. We analyzed the downstream factors of  $\beta$ -catenin and found that the protein levels of TCF4 and pygopus2 were reduced by **4r** and resveratrol in CRC cells (Figure 6E). RT-PCR assay suggested that **4r** strongly inhibited the transcription of Wnt target genes. It also inhibited TCF4 genes but had no significant effects on pygopus2 genes, which suggested that these new fluorinated *N,N*-dialkylaminostilbenes inhibited Wnt/mediated transcription at multiple levels (Figure 6F).

## DISCUSSION

The Wnt pathway is an important drug target for human cancers, particularly CRC.  $\beta$ -Catenin levels are significantly increased in CRC cells because of the mutation of APC or  $\beta$ -catenin. Several small molecular inhibitors are reported to promote  $\beta$ -catenin degradation by inhibiting tankyrase.<sup>11,12</sup> Although these inhibitors are useful in studying Wnt signaling in normal cells, they are less effective in CRC cells containing  $\beta$ -catenin mutations. Moreover, these inhibitors have not been tested in tumor models in vivo. Their potential toxicity remains an indeterminate concern if these compounds were used in clinical applications.

For example, tankyrase is essential for embryonic development, and deficiency in both tankyrase 1 and 2 resulted in embryonic lethality by day 10.<sup>23</sup> The tankyrase inhibitors induced damage to the intestinal tract, although this side effect is reversible probably depending on the dosage.<sup>15</sup> Many anticancer agents derived from plants, including resveratrol, have been suggested to inhibit Wnt signaling, but the mechanisms are not clear.<sup>21,24–27</sup> Resveratrol has been suggested to induce  $\beta$ -catenin degradation and inhibits its nuclear localization in CRC cells,<sup>21</sup> but it increases  $\beta$ -catenin stability and nuclear accumulation in multipotent mesenchymal cells.<sup>28</sup> It has been suggested that resveratrol inhibits GSK-3 at low concentration and activates GSK-3 at high concentration in endothelial cells. It is possible that resveratrol regulates Wnt pathway depending on cell context.<sup>29</sup> In this study, we found that resveratrol and the more potent pterostilbene inhibited Wnt signaling downstream of  $\beta$ -catenin and inhibited the proliferation of CRC cells (Figure 1), but both agents are only active at 10–100  $\mu\text{M}$ . We have synthesized and screened many analogues and identified several fluorinated *N,N*-dialkylaminostilbenes as new and potent Wnt inhibitors.

Initial findings that resveratrol and other hydroxyl- or methoxy-substituted stilbenes produced greater than 50% Wnt inhibition at 10–100  $\mu\text{M}$  (data not shown) using a luciferase-based assay led to a search for modified stilbenes with improved potency. Because the luciferase-based assay was prone to false positives, an unambiguous but more laborious assay involving

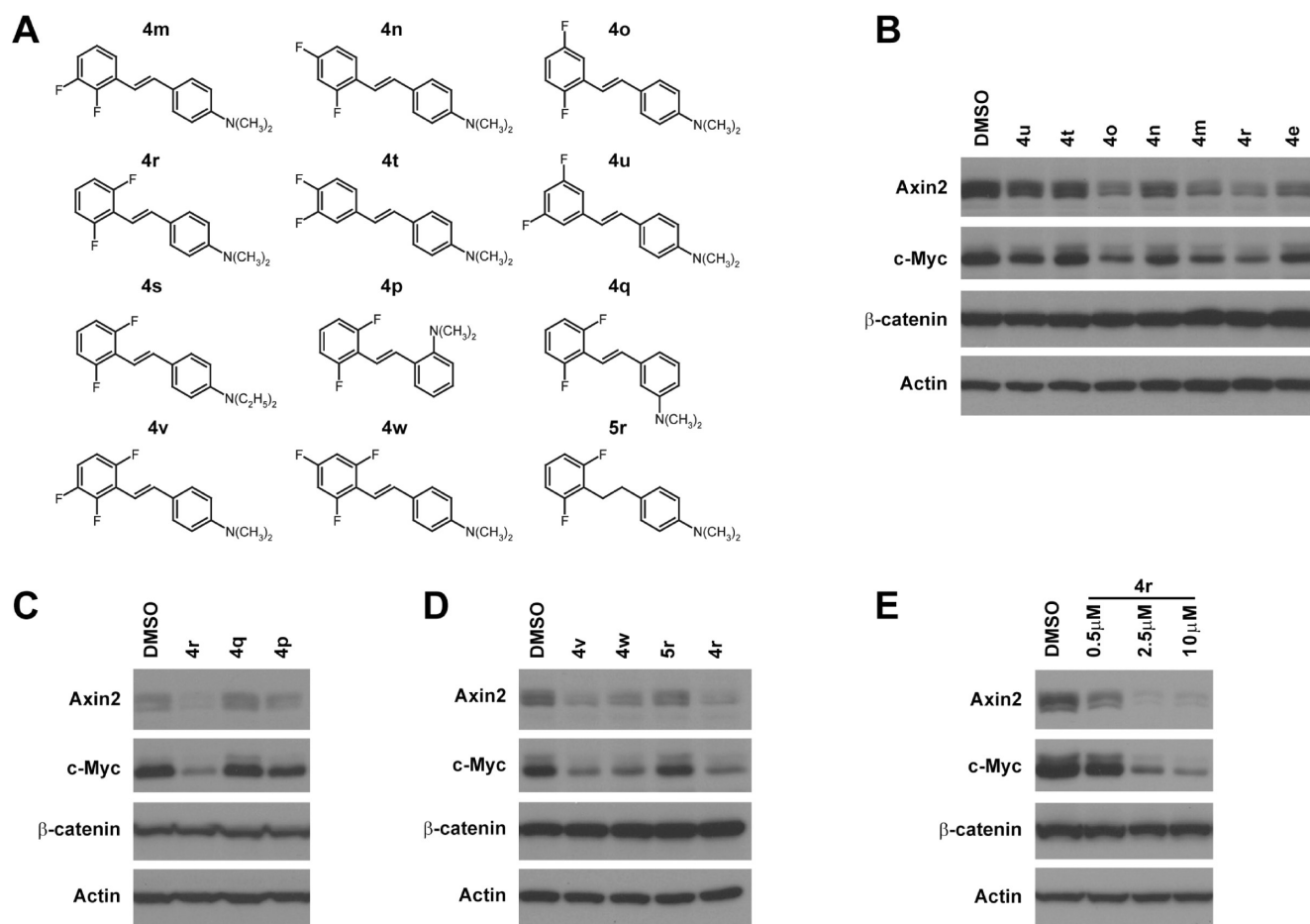


**Figure 4.** 4-(2,6-Difluorostyryl)-*N,N*-dimethylaniline (**4r**) is a potent Wnt inhibitor. (A) Chemical structures of difluorinated *N,N*-dialkylaminostilbenes. (B) Difluorinated *N,N*-dimethylaminostilbenes, **4o**, **4m**, and **4r**, repress Wnt target genes at 10  $\mu$ M. (C) The ortho and meta isomers of *N,N*-dimethylamino analogues (**4p** and **4q**) are not as active as the para isomer (**4r**). (D) Trifluorinated *N,N*-dimethylaminostilbenes (**4v** and **4w**) are active Wnt inhibitors but have no particular advantage over **4r**. The carbon-carbon double bond in **4r** is necessary for its activity. (E) **4r** represses Wnt target genes at 0.5  $\mu$ M.

Western blots to measure Wnt target protein levels was employed. With this assay system, a broad spectrum of stilbenes were screened and the fluorinated *N,N*-dialkylaminostilbenes **4** proved to be the most promising. Efforts to replace one of the aryl rings with various heterocyclic and polyaromatic systems or to modify the *N,N*-dimethylamino substituent with other alkyl or aryl groups led to a loss of activity. The inclusion of fluorine substituents, particularly a fluorine ortho to the stilbene double bond, not only improved the solubility of the stilbenes but also led finally to (*E*)-4-(2,6-difluorostyryl)-*N,N*-dimethylaniline (**4r**) as the most active compound in this series.

The stilbene **4r** was 10- to 100-fold more potent than resveratrol and pterostilbene in Western blot and cell proliferation assays (Figure 4). Stilbene **4r** also repressed the growth of LS174 tumor xenografts, suggesting that this agent inhibits Wnt signaling in vivo (Figure 5). LS174 and HCT116 cells contain a  $\beta$ -catenin mutation (serine 45 deletion), and this mutation prevents  $\beta$ -catenin phosphorylation by CKI $\alpha$  and GSK-3, thus preventing  $\beta$ -catenin degradation. Upstream signals in Wnt signaling can no longer regulate  $\beta$ -catenin levels in these cells, and agents targeting upstream of signaling events are ineffective (data not show). Since these new analogues inhibit Wnt signaling in LS174 and HCT116 cells, they must inhibit Wnt signaling downstream of  $\beta$ -catenin. This is consistent with the fact that

these agents did not reduce  $\beta$ -catenin levels and that they inhibited both Wnt-induced and LiCl-induced reporter activities. Since Lgr5 and several other Wnt targets are markers for intestinal stem cell and CRC stem cells,<sup>30</sup> it is possible that these agents inhibit cancer stem cells. Other than CRCs, Wnt signaling is required for tumorigenesis of many other types of cancer. For example,  $\beta$ -catenin mutations are frequent in hepatocellular carcinoma and hepatoblastoma.<sup>3,5</sup> These fluorinated *N,N*-dialkylaminostilbenes **4** that inhibit Wnt targets in CRC may also inhibit other human cancers.

Using fluorescence techniques, aided by the fact that these fluorinated *N,N*-dialkylaminostilbenes themselves were fluorescent, we found that these agents are cell permeable and are localized in both the nucleus and the cytoplasm. After 12 h, the nuclear levels of these agents are decreased (Figure 6), probably by a drug-exporting mechanism.<sup>31</sup> After **4r** treatment, the  $\beta$ -catenin levels in the cytoplasmic and nuclear fractions were slightly increased but significant amounts of  $\beta$ -catenin were still localized in the nucleus. The strong inhibition displayed by these agents on  $\beta$ -catenin targets led to the hypothesis that these agents may inhibit Wnt signaling other than at  $\beta$ -catenin levels and localization. We analyzed the nuclear factors of the Wnt pathway and found that the protein levels of TCF4 and pygopus2 were decreased. Both TCF4 and pygopus2 are required for Wnt-mediated transcription,<sup>32</sup>

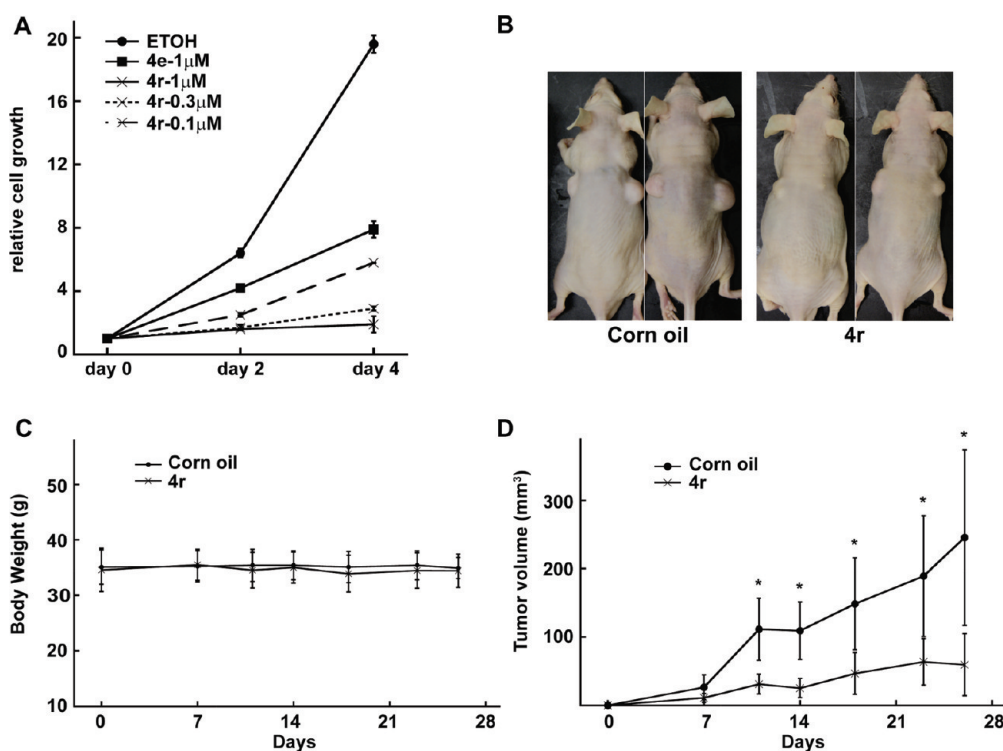


**Figure 5.** Effects of fluorinated *N,N*-dialkylaminostilbenes on CRC cell proliferation in vitro and in vivo. (A) **4r** inhibits CRC cell proliferation at 0.1 μM. (B) LS174 CRC cells ( $2 \times 10^6$ ) were injected subcutaneously into both flanks of athymic nude mice. (B) Representative nude mice treated with **4r** or corn oil. (C) Body weights of nude mice treated with **4r** and corn oil. (D) The tumor sizes were measured twice a week. The tumor volumes were calculated using the formula  $V = \frac{1}{2}LW^2$  (mm<sup>3</sup>). The xenograft tumors treated with **4r** grew to a lesser extent than the xenograft tumors treated with just corn oil. Statistical significance was calculated by the Student's *t* test (\*,  $p < 0.05$ ).

indicating that these agents inhibit the transcriptional initiation complex in the Wnt signaling. The mRNA levels of Wnt target genes, *Axin2* and *c-Myc*, were significantly decreased (Figure 6E). TCF4 is a potential Wnt target gene.<sup>33</sup> The transcription of TCF4 but not *pygopus2* was inhibited by **4r**, suggesting that these fluorinated *N,N*-dialkylaminostilbenes **4** may regulate  $\beta$ -catenin activity through multiple mechanisms. Studies are underway to determine the direct target or targets of these promising new agents. In summary, we have identified fluorinated *N,N*-dialkylaminostilbenes as a family of new and potent stilbene analogues that inhibit Wnt pathway and CRC. This work will lead to further exploration of potential novel mechanisms and novel applications of these agents in human diseases.

## EXPERIMENTAL PROCEDURES

**Chemistry.** Chemicals were purchased from Sigma Aldrich, MP Biomedical (**4c**), or TCI (**4d**) or were synthesized according to literature procedures. Solvents were used from commercial vendors without further purification unless otherwise noted. Nuclear magnetic resonance spectra were determined in acetone-*d*<sub>6</sub> using a Varian instrument (<sup>1</sup>H, 400 MHz; <sup>13</sup>C, 100 MHz unless otherwise noted). LRMS electron-impact (EI) ionization mass spectra were recorded at 70 eV on a ThermoFinnigan PolarisQ (ion trap mass spectrometer). Samples were introduced via a heatable direct probe inlet. Purity of compounds was >95% as established by combustion analyses. Elemental analyses were conducted by Atlantic Microlabs, Inc., Norcross, GA. Compounds were chromatographed on preparative layer Merck silica gel F254 unless otherwise indicated.

**General Procedure A.** To 1.5 mmol of triphenylphosphonium bromide **1** suspended in 4 mL of anhydrous THF at  $-78^\circ\text{C}$  was added

2.25 mmol (1.5 equiv) of *n*-BuLi (1.6 M in hexane). The mixture was allowed to warm to  $25^\circ\text{C}$  for 30 min, and 2.25 mmol of aldehyde **3** in 1 mL of anhydrous THF was added. The mixture was stirred for 24 h, diluted with CH<sub>2</sub>Cl<sub>2</sub>, washed with saturated NH<sub>4</sub>Cl solution, and dried over anhydrous MgSO<sub>4</sub>. The product was purified by chromatography and/or recrystallization as noted for individual stilbenes **4** listed below.

**General Procedure B.** To a solution of 1.5 mmol of diethyl phosphonate **2** in 4 mL of anhydrous DMF at  $0^\circ\text{C}$  was added 2.25 mmol (1.5 equiv) of NaH (washed with hexanes to remove oil). The mixture was stirred for 20 min, and 1.5 mmol of aldehyde **3** in 1 mL of anhydrous DMF was added dropwise. The mixture was stirred for 24 h at  $25^\circ\text{C}$ , quenched with ice, extracted with CH<sub>2</sub>Cl<sub>2</sub>, and dried over anhydrous MgSO<sub>4</sub>. The product was purified by chromatography and/or recrystallization as noted for individual stilbenes **4** listed below.

**(E)-4-Hydroxystilbene (4a).** To 210 mg (1 mmol) of (*E*)-4-methoxystilbene (**4b**) in 7 mL of CH<sub>2</sub>Cl<sub>2</sub> was added 1.28 mL of 1 M BBr<sub>3</sub> (1.3 mmol) in dichloromethane at  $-10^\circ\text{C}$ . The mixture was stirred for 4 h at  $-5^\circ\text{C}$  and quenched by pouring into cold water. The product was extracted with CH<sub>2</sub>Cl<sub>2</sub>, dried over anhydrous MgSO<sub>4</sub>, and chromatographed using 1:10 CH<sub>3</sub>OH/CH<sub>2</sub>Cl<sub>2</sub> to afford 85 mg (43%) of **4a**. Mp  $184\text{--}185^\circ\text{C}$  (lit.<sup>34</sup>  $186^\circ\text{C}$ ).

**(E)-4-Methoxystilbene (4b).** Procedure B was used. Yield 87%. Colorless crystals: mp  $136\text{--}137^\circ\text{C}$  (lit.<sup>34</sup>  $136\text{--}138^\circ\text{C}$ ).

**(E)-4-(2-Fluorostyryl)-*N,N*-dimethylaniline (4e).** Procedure B was used. Yield 84%. Light yellow crystals from acetonitrile. Mp  $124\text{--}126^\circ\text{C}$ . <sup>1</sup>H NMR:  $\delta$  7.73–7.68 (m, 1H), 7.46 (d, 2H,  $J = 8.8$  Hz), 7.26–7.08 (m, 3H), 7.22 (d, 1H,  $J = 16.4$  Hz), 7.09 (d, 1H,  $J = 16.8$  Hz), 6.75 (d, 2H,  $J = 9.2$  Hz), 2.98 (s, 6H). <sup>13</sup>C NMR:  $\delta$  160.18 (d,  $J = 245.9$  Hz), 150.85, 131.67 (d,  $J = 4.6$  Hz), 128.08 (d,  $J = 8.4$  Hz), 127.93, 126.8 (d,  $J = 4.5$  Hz), 126.14 (d,  $J = 12.1$  Hz), 125.46, 124.59 (d,  $J = 3.1$  Hz), 115.64 (d,  $J = 22.0$  Hz), 115.49 (d,  $J = 4.6$  Hz), 112.44, 39.69. MS:  $m/z$  (9)

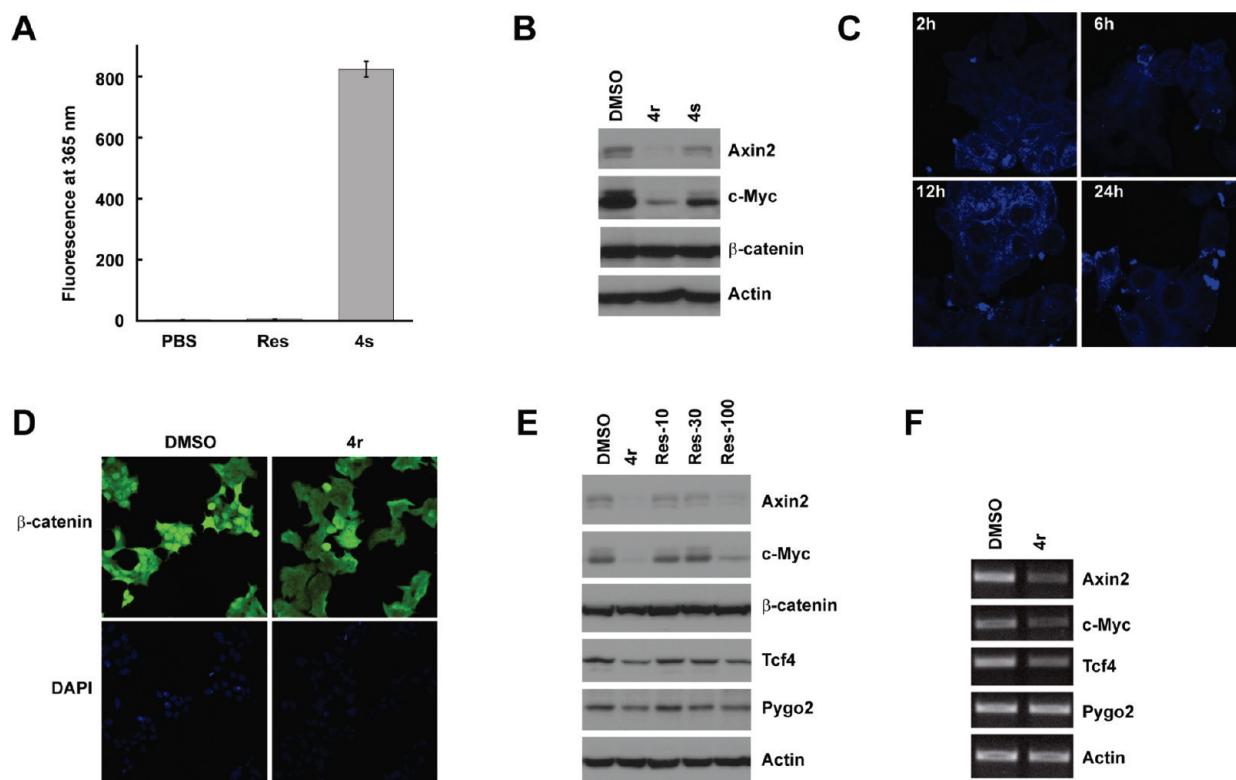


**Figure 6.** Potential mechanisms of fluorinated *N,N*-dialkylaminostilbenes in Wnt inhibition. (A) **4s** has strong fluorescence at 365 nm (detected by Promega GloMax luminometer). (B) **4s** is an active Wnt inhibitor. (C) **4s** was incubated with LS174 CRC cells for 2, 6, 12, and 24 h. The localization of **4s** was analyzed by confocal fluorescence microscopy. (D) Immunofluorescence staining of  $\beta$ -catenin in LS174 cells treated with DMSO or **4r**. Nuclei were stained with DAPI. (E) **4r** (10  $\mu$ M) and resveratrol (100  $\mu$ M) reduced the protein levels of Wnt/ $\beta$ -catenin targets in LS174 cells. **4r** and resveratrol also reduced the protein levels of TCF4 and pygopus2 but not  $\beta$ -catenin. (F) **4r** repressed the transcription of Wnt target genes.

241 (100), 240 (74), 225 (32), 197 (20), 196 (20), 177 (18), 176 (13). Anal. Calcd for  $C_{16}H_{16}FN$ : C, 79.64; H, 6.68. Found: C, 79.77; H, 6.80.

**(E)-4-(3-Fluorostyryl)-*N,N*-dimethylaniline (4f).** Procedure B was used. Yield 65%. Light yellow crystals from acetonitrile. Mp 147–148  $^{\circ}C$ .  $^1H$  NMR:  $\delta$  7.42 (d, 2H,  $J = 8.4$  Hz), 7.35–7.25 (m, 3H), 7.17 (d, 1H,  $J = 16.4$  Hz), 6.96 (d, 1H,  $J = 16.8$  Hz), 6.93–6.88 (m, 1H), 6.72 (d, 2H,  $J = 8.8$  Hz), 2.95 (s, 6H).  $^{13}C$  NMR:  $\delta$  163.47 (d,  $J = 241.4$  Hz), 150.82, 141.36 (d,  $J = 7.6$  Hz), 130.66, 130.42 (d,  $J = 8.4$  Hz), 127.97, 125.22, 122.63 (d,  $J = 2.2$  Hz), 122.24 (d,  $J = 2.2$  Hz), 113.12 (d,  $J = 21.3$  Hz), 112.43, 111.96 (d,  $J = 22.0$  Hz), 39.69. MS:  $m/z$  (%) 241 (100), 240 (69), 225 (25), 197 (20), 196 (18), 177 (16), 176 (10). Anal. Calcd for  $C_{16}H_{16}FN$ : C, 79.64; H, 6.68. Found: C, 79.86; H, 6.67.

**(E)-4-(4-Fluorostyryl)-*N,N*-dimethylaniline (4g).** Procedure B was used. Yield 64%. Light yellow crystals from acetonitrile. Mp 197–198  $^{\circ}C$  (lit.<sup>35</sup> 194–195  $^{\circ}C$ ). Anal. Calcd for  $C_{16}H_{16}FN$ : C, 79.64; H, 6.68. Found: C, 79.85; H, 6.64.

**(E)-4-(2-Fluorostyryl)-*N,N*-diethylaniline (4h).** Procedure B was used. Yield 51%. Light yellow crystals from hexane. Mp 78–79  $^{\circ}C$ .  $^1H$  NMR:  $\delta$  7.69–7.65 (m, 1H), 7.40 (d, 2H,  $J = 8.8$  Hz), 7.24–7.07 (m, 3H), 7.20 (d, 1H,  $J = 16.4$  Hz), 7.04 (d, 1H,  $J = 16.4$  Hz), 6.71 (d, 2H,  $J = 8.8$  Hz), 3.42 (q, 4H,  $J = 7.2$  Hz), 1.16 (t, 6H,  $J = 7.2$  Hz).  $^{13}C$  NMR:  $\delta$  160.13 (d,  $J = 242.2$  Hz), 148.04, 131.73 (d,  $J = 4.5$  Hz), 128.24, 127.91 (d,  $J = 7.6$  Hz), 126.70 (d,  $J = 4.5$  Hz), 126.27 (d,  $J = 11.4$  Hz), 124.57 (d,  $J = 3.8$  Hz), 124.49, 115.62 (d,  $J = 22.0$  Hz), 114.82 (d,  $J = 3.8$  Hz), 111.76, 44.19, 12.21. MS:  $m/z$  (%) 269 (34), 255 (19), 254 (100), 226 (22), 225 (20), 197 (16), 196 (17). Anal. Calcd for  $C_{18}H_{20}FN$ : C, 80.26; H, 7.48. Found: C, 80.07; H, 7.61.

**(E)-4-(2-Fluorostyryl)-*N,N*-diphenylaniline (4i).** Procedure B was used. Yield 60%. Light yellow crystals from hexane. Mp 114–115  $^{\circ}C$ .  $^1H$  NMR:  $\delta$  7.77–7.73 (m, 1H), 7.54 (d, 2H,  $J = 8.4$  Hz),

7.34–7.06 (m, 15H), 7.02 (d, 2H,  $J = 8.8$  Hz).  $^{13}C$  NMR:  $\delta$  160.39 (d,  $J = 245.9$  Hz), 148.00, 147.73, 131.58, 130.87 (d,  $J = 4.5$  Hz), 129.63, 128.90 (d,  $J = 8.3$  Hz), 127.88, 127.23 (d,  $J = 3.8$  Hz), 125.58 (d,  $J = 12.0$  Hz), 124.75, 124.71, 123.53, 123.25, 118.78 (d,  $J = 3.8$  Hz), 115.76 (d,  $J = 22.0$  Hz). MS:  $m/z$  (%) 365 (100), 364 (12), 254 (13). Anal. Calcd for  $C_{26}H_{20}FN$ : C, 85.45; H, 5.52. Found: C, 85.59; H, 5.69.

**(E)-1-(4-(2-Fluorostyryl)phenyl)-4-methylpiperazine (4j).** Procedure B was used. Yield 65%. Light yellow crystals from acetonitrile. Mp 142–144  $^{\circ}C$ .  $^1H$  NMR:  $\delta$  7.72–7.69 (m, 1H), 7.48 (d, 2H,  $J = 8.8$  Hz), 7.28–7.09 (m, 3H), 7.24 (d, 1H,  $J = 16.4$  Hz), 7.13 (d, 1H,  $J = 16.4$  Hz), 6.96 (d, 2H,  $J = 8.8$  Hz), 3.22 (t, 4H,  $J = 5.2$  Hz), 2.48 (t, 4H,  $J = 5.2$  Hz), 2.54 (s, 3H).  $^{13}C$  NMR:  $\delta$  160.27 (d,  $J = 245.2$  Hz), 151.59, 131.34 (d,  $J = 5.3$  Hz), 128.42 (d,  $J = 8.4$  Hz), 127.97, 127.81, 126.98 (d,  $J = 3.8$  Hz), 125.90 (d,  $J = 12.1$  Hz), 126.62 (d,  $J = 3.8$  Hz), 116.85 (d,  $J = 3.8$  Hz), 115.69 (d,  $J = 22.0$  Hz), 115.46, 55.09, 48.34, 45.70. MS:  $m/z$  (%) 296 (100), 281 (42), 226 (24), 211 (46), 197 (28), 196 (42), 177 (28). Anal. Calcd for  $C_{19}H_{21}FN_2$ : C, 77.00; H, 7.14. Found: C, 77.22; H, 7.49.

**(E)-4-(2-Fluorostyryl)-*N,N*-dimethylnaphthalen-1-amine (4k).** Procedure B was used. Yield 18%. Yellow crystals from hexane/ $Et_2O$ . Mp 56–58  $^{\circ}C$ .  $^1H$  NMR:  $\delta$  8.33–8.27 (m, 2H), 8.09 (d, 1H,  $J = 16.4$  Hz), 7.95–7.91 (m, 1H), 7.80 (d, 1H,  $J = 8.0$  Hz), 7.58–7.52 (m, 2H), 7.36–7.15 (m, 4H), 7.28 (d, 1H,  $J = 16.4$  Hz), 2.90 (s, 6H).  $^{13}C$  NMR:  $\delta$  160.49 (d,  $J = 246.7$  Hz), 151.66, 132.85, 129.41, 129.10 (d,  $J = 8.4$  Hz), 128.92, 128.38 (d,  $J = 4.6$  Hz), 127.67 (d,  $J = 3.8$  Hz), 126.27, 125.78 (d,  $J = 12.2$  Hz), 125.17, 124.92, 124.74 (d,  $J = 3.0$  Hz), 124.25, 124.03, 121.75 (d,  $J = 3.8$  Hz), 115.78 (d,  $J = 22.0$  Hz), 114.19, 44.62. MS:  $m/z$  (%) 291 (100), 290 (28), 276 (70), 261 (40), 247 (22), 246 (15). Anal. Calcd for  $C_{20}H_{18}FN$ : C, 82.45; H, 6.23. Found: C, 82.42; H, 6.22.

**(E)-2-(4-(2-Fluorostyryl)phenyl)-1-methyl-1H-imidazole (4l).** Procedure B was used. Yield 47%. Colorless crystals from hexane. Mp 60–61 °C.  $^1\text{H}$  NMR:  $\delta$  7.82–7.78 (m, 1H), 7.65 (d, 1H,  $J$  = 16.0 Hz), 7.35–7.29 (m, 1H), 7.26 (d, 1H,  $J$  = 16.0 Hz), 7.22–7.13 (m, 2H), 7.08 (d, 1H,  $J$  = 1.2 Hz), 6.96 (d, 1H,  $J$  = 0.8 Hz), 3.81 (s, 3H).  $^{13}\text{C}$  NMR:  $\delta$  160.65 (d,  $J$  = 246.7 Hz), 145.39, 129.53 (d,  $J$  = 8.3 Hz), 128.89, 127.66 (d,  $J$  = 3.0 Hz), 124.98 (d,  $J$  = 11.4 Hz), 124.71 (d,  $J$  = 3.8 Hz), 122.73 (d,  $J$  = 3.8 Hz), 122.18, 116.99 (d,  $J$  = 5.3 Hz), 115.83 (d,  $J$  = 22.0 Hz), 32.04. MS:  $m/z$  (%) 202 (17), 201 (59), 186 (20), 183 (100), 168 (25), 146 (16), 128 (17). Anal. Calcd for  $\text{C}_{12}\text{H}_{11}\text{FN}_2$ : C, 71.27; H, 5.48. Found: C, 71.24; H, 5.61.

**(E)-4-(2,3-Difluorostyryl)-*N,N*-dimethylaniline (4m).** Procedure A was used. Yield 88%. Yellow crystals. Mp 132–133 °C.  $^1\text{H}$  NMR:  $\delta$  7.50–7.47 (m, 1H), 7.45 (d, 2H,  $J$  = 9.2 Hz), 7.24 (d, 1H,  $J$  = 16.4 Hz), 7.16–7.06 (m, 2H), 7.03 (d, 1H,  $J$  = 16.4 Hz), 6.73 (d, 2H,  $J$  = 8.8 Hz), 2.96 (s, 6H).  $^{13}\text{C}$  NMR:  $\delta$  151.01 (dd,  $J$  = 243.6 Hz), 147.87 (dd,  $J$  = 246.3 Hz), 133.18 (d,  $J$  = 5.3 Hz), 128.69 (d,  $J$  = 9.1 Hz), 128.19, 124.95, 124.57 (d,  $J$  = 7.6 Hz), 124.53 (d,  $J$  = 7.6 Hz), 121.78 (t,  $J$  = 3.0 Hz), 114.65 (d,  $J$  = 17.4 Hz), 114.24 (t,  $J$  = 3.8 Hz), 112.37, 39.64. MS:  $m/z$  (%) 259 (100), 258 (78), 243 (25), 214 (16), 195 (16). Anal. Calcd for  $\text{C}_{16}\text{H}_{15}\text{F}_2\text{N}$ : C, 74.11; H, 5.83. Found: C, 74.01; H, 5.71.

**(E)-4-(2,4-Difluorostyryl)-*N,N*-dimethylaniline (4n).** Procedure B was used. Yield 58%. Yellow crystals from acetonitrile. Mp 139–140 °C.  $^1\text{H}$  NMR:  $\delta$  7.77–7.71 (m, 1H), 7.44 (d, 2H,  $J$  = 8.4 Hz), 7.17 (d, 1H,  $J$  = 16.4 Hz), 7.01 (d, 1H,  $J$  = 16.4 Hz), 7.02–6.97 (m, 2H), 6.75 (d, 2H,  $J$  = 9.2 Hz), 2.98 (s, 6H).  $^{13}\text{C}$  NMR:  $\delta$  161.64 (dd,  $J$  = 245.2 Hz), 159.99 (dd,  $J$  = 248.9 Hz, 248.2 Hz), 150.87, 131.54 (dd,  $J$  = 4.5 Hz), 127.89, 125.34, 122.84 (dd,  $J$  = 12.1 Hz), 114.56 (t,  $J$  = 1.6 Hz), 112.43, 111.73 (dd,  $J$  = 21.3 Hz), 103.85 (t,  $J$  = 26.5 Hz,  $J$  = 25.8 Hz), 39.68. MS:  $m/z$  (%) 259 (100), 258 (71), 243 (30), 215 (15), 195 (14). Anal. Calcd for  $\text{C}_{16}\text{H}_{15}\text{F}_2\text{N}$ : C, 74.11; H, 5.83. Found: C, 74.25; H, 5.77.

**(E)-4-(2,5-Difluorostyryl)-*N,N*-dimethylaniline (4o).** Procedure A was used. Yield 77%. Yellow crystals. Mp 146–147 °C.  $^1\text{H}$  NMR:  $\delta$  7.51–7.46 (m, 3H), 7.28 (d, 1H,  $J$  = 16.4 Hz), 7.18–7.12 (m, 1H), 7.03 (d, 1H,  $J$  = 16.4 Hz), 7.00–6.95 (m, 1H), 6.76 (d, 2H,  $J$  = 8.8 Hz), 2.99 (s, 6H).  $^{13}\text{C}$  NMR:  $\delta$  159.28 (dd,  $J$  = 236.0 Hz), 156.22 (dd,  $J$  = 241.4 Hz), 151.09, 133.04 (d,  $J$  = 3.8 Hz), 128.21, 124.94, 117.01 (d,  $J$  = 25.8 Hz), 116.92 (d,  $J$  = 25.1 Hz), 114.12 (d,  $J$  = 25.1 Hz), 114.03 (d,  $J$  = 24.3 Hz), 112.37, 112.12 (d,  $J$  = 4.5 Hz), 39.64. MS:  $m/z$  (%) 259 (100), 258 (84), 243 (29), 215 (18), 195 (17). Anal. Calcd for  $\text{C}_{16}\text{H}_{15}\text{F}_2\text{N}$ : C, 74.11; H, 5.83. Found: C, 74.63; H, 5.90.

**(E)-2-(2,6-Difluorostyryl)-*N,N*-dimethylaniline (4p).** Procedure B was used. Yield 92%. Yellow oil.  $^1\text{H}$  NMR:  $\delta$  7.78 (d, 1H,  $J$  = 16.8 Hz), 7.65 (dd, 1H,  $J$  = 1.6 Hz), 7.36–7.26 (m, 2H), 7.12–7.03 (m, 4H), 7.09 (d, 1H,  $J$  = 17.2 Hz), 2.74 (s, 6H).  $^{13}\text{C}$  NMR:  $\delta$  161.10 (d,  $J$  = 248.2 Hz), 161.02 (d,  $J$  = 248.2 Hz), 152.77, 133.80 (t,  $J$  = 8.3 Hz,  $J$  = 7.6 Hz), 131.25, 129.19, 128.59 (t,  $J$  = 11.4 Hz,  $J$  = 10.6 Hz), 126.72, 122.65, 118.46, 115.31 (t,  $J$  = 15.2 Hz,  $J$  = 15.9 Hz), 113.84, 111.95 (d,  $J$  = 19.7 Hz), 111.89 (d,  $J$  = 19.0 Hz), 44.31. MS:  $m/z$  (%) 259 (100), 258 (14), 132 (8). Anal. Calcd for  $\text{C}_{16}\text{H}_{15}\text{F}_2\text{N}$ : C, 74.11; H, 5.83. Found: C, 74.38; H, 5.79.

**(E)-3-(2,6-Difluorostyryl)-*N,N*-dimethylaniline (4q).** Procedure B was used. Yield 53%. Colorless crystals from hexane. Mp 69–71 °C.  $^1\text{H}$  NMR:  $\delta$  7.38 (d, 1H,  $J$  = 16.8 Hz), 7.33–7.26 (m, 1H), 7.19 (t, 1H,  $J$  = 8.4 Hz,  $J$  = 8.0 Hz), 7.11 (d, 1H,  $J$  = 17.2 Hz), 7.03 (dd, 2H,  $J$  = 8.4 and 8.8 Hz), 6.93–6.91 (m, 2H), 6.72–6.69 (m, 1H), 2.96 (s, 6H).  $^{13}\text{C}$  NMR:  $\delta$  161.06 (d,  $J$  = 248.2 Hz), 160.98 (d,  $J$  = 248.2 Hz), 151.38, 138.03, 136.83 (t,  $J$  = 7.6 Hz,  $J$  = 8.3 Hz), 129.46, 128.70 (t,  $J$  = 10.6 Hz,  $J$  = 11.4 Hz), 114.87 (t,  $J$  = 16 Hz), 114.81, 114.09, 112.98, 111.94 (d,  $J$  = 19.7 Hz), 111.88 (d,  $J$  = 19.0 Hz), 111.21, 39.93. MS:  $m/z$  (%) 259 (100), 258 (52), 239 (31), 238 (33), 223 (16), 222 (37). Anal. Calcd for  $\text{C}_{16}\text{H}_{15}\text{F}_2\text{N}$ : C, 74.11; H, 5.83. Found: C, 74.30; H, 5.78.

**(E)-4-(2,6-Difluorostyryl)-*N,N*-dimethylaniline (4r).** Procedure B was used. Yield 94%. Colorless crystals from hexane. Mp 112–113 °C.  $^1\text{H}$  NMR:  $\delta$  7.45 (d, 2H,  $J$  = 8.4 Hz), 7.35 (d, 1H,  $J$  = 16.8 Hz), 7.27–7.20 (m, 1H), 7.01 (dd, 2H,  $J$  = 8.4 and 8.8 Hz), 6.91 (1H, d,  $J$  = 16.8 Hz), 6.75 (d, 2H,  $J$  = 9.2 Hz), 2.98 (s, 6H).  $^{13}\text{C}$  NMR:  $\delta$  160.86 (d,  $J$  = 247.4 Hz), 160.78 (d,  $J$  = 248.3 Hz), 151.10, 135.99 (t,  $J$  = 8.3 Hz), 127.97, 127.57 (t,  $J$  = 11.3 Hz), 125.41, 115.50 (t,  $J$  = 16.0 Hz), 112.40, 111.82 (d,  $J$  = 19.0 Hz), 111.76 (d,  $J$  = 19.0 Hz), 109.73, 39.65. MS:  $m/z$  (%) 259 (100), 258 (71), 243 (25), 195 (11). Anal. Calcd for  $\text{C}_{16}\text{H}_{15}\text{F}_2\text{N}$ : C, 74.11; H, 5.83. Found: C, 74.08; H, 5.79.

**(E)-4-(2,6-Difluorostyryl)-*N,N*-diethylaniline (4s).** Procedure B was used. Yield 57%. Yellow crystals from hexane. Mp 70–71 °C.  $^1\text{H}$  NMR:  $\delta$  7.43 (d, 2H,  $J$  = 8.4 Hz), 7.34 (d, 1H,  $J$  = 16.8 Hz), 7.27–7.20 (m, 1H), 7.01 (dd, 2H,  $J$  = 8.4 Hz), 6.89 (d, 1H,  $J$  = 16.8 Hz), 6.72 (d, 2H,  $J$  = 8.8 Hz), 3.43 (q, 4H,  $J$  = 7.2 Hz), 1.16 (t, 6H,  $J$  = 7.2 Hz).  $^{13}\text{C}$  NMR:  $\delta$  160.83 (d,  $J$  = 246.7 Hz), 160.75 (d,  $J$  = 247.4 Hz), 148.30, 136.07 (t,  $J$  = 8.3 Hz), 128.29, 127.37 (t,  $J$  = 10.6 Hz), 124.45, 115.62 (t,  $J$  = 16.0 Hz), 111.81 (d,  $J$  = 19.0 Hz), 111.74 (d,  $J$  = 19.8 Hz), 111.73, 109.07, 44.20, 12.20. MS:  $m/z$  (%) 287 (44), 272 (100), 244 (21), 243 (15). Anal. Calcd for  $\text{C}_{18}\text{H}_{19}\text{F}_2\text{N}$ : C, 75.24; H, 6.66. Found: C, 75.12; H, 6.79.

**(E)-4-(3,4-Difluorostyryl)-*N,N*-dimethylaniline (4t).** Procedure A was used. Yield 59%. Yellow crystals from hexane. Mp 159–160 °C.  $^1\text{H}$  NMR:  $\delta$  7.50–7.44 (m, 1H), 7.41 (d, 2H,  $J$  = 8.8 Hz), 7.32–7.28 (m, 1H), 7.27–7.20 (m, 1H), 7.11 (d, 1H,  $J$  = 16.0 Hz), 6.92 (d, 1H,  $J$  = 16.4 Hz), 6.71 (d, 2H,  $J$  = 8.8 Hz), 2.95 (s, 6H).  $^{13}\text{C}$  NMR:  $\delta$  150.82, 150.56 (dd,  $J$  = 243.9 Hz), 150.50, 148.98 (dd,  $J$  = 244.3 Hz), 136.59, 130.55 (d,  $J$  = 3.0 Hz), 127.91, 125.16, 122.71 (d,  $J$  = 6.1 Hz), 122.68 (d,  $J$  = 6.1 Hz), 121.68 (d,  $J$  = 2.3 Hz), 117.49 (d,  $J$  = 17.4 Hz), 113.96 (d,  $J$  = 17.5 Hz), 112.43, 39.68. MS:  $m/z$  (%) 259 (100), 258 (82), 243 (36), 215 (22), 195 (16). Anal. Calcd for  $\text{C}_{16}\text{H}_{15}\text{F}_2\text{N}$ : C, 74.11; H, 5.83. Found: C, 74.24; H, 5.79.

**(E)-4-(3,5-Difluorostyryl)-*N,N*-dimethylaniline (4u).** Procedure A was used. Yield 51%. Yellow crystals. Mp 136–137 °C (lit.<sup>36</sup> 139–141 °C). Anal. Calcd for  $\text{C}_{16}\text{H}_{15}\text{F}_2\text{N}$ : C, 74.11; H, 5.83. Found: C, 74.38; H, 5.70.

**(E)-*N,N*-Dimethyl-4-(2,3,6-trifluorostyryl)aniline (4v).** Procedure B was used. Yield 45%. Light yellow crystals from hexane. Mp 91–92 °C.  $^1\text{H}$  NMR:  $\delta$  7.48 (d, 2H,  $J$  = 9.2 Hz), 7.39 (d, 1H,  $J$  = 16.8 Hz), 7.22–7.14 (m, 1H), 7.06–7.00 (m, 1H), 6.89 (d, 1H,  $J$  = 16.8 Hz), 6.76 (d, 2H,  $J$  = 8.0 Hz), 3.00 (s, 6H).  $^{13}\text{C}$  NMR:  $\delta$  157.35–154.83 (m, 1C), 151.31, 149.49–146.37 (m, 2C), 137.17 (t,  $J$  = 8.4 Hz), 128.23, 124.89, 117.43 (dd,  $J$  = 17.4 Hz,  $J$  = 16.7 Hz), 114.01 (dd,  $J$  = 18.9 Hz,  $J$  = 19.8 Hz), 112.33, 111.39–111.02 (m, 1C), 108.99, 39.59. MS:  $m/z$  (%) 277 (100), 276 (83), 261 (24), 214 (16), 213 (12). Anal. Calcd for  $\text{C}_{16}\text{H}_{14}\text{F}_3\text{N}$ : C, 69.30; H, 5.09. Found: C, 69.50; H, 4.97.

**(E)-*N,N*-Dimethyl-4-(2,4,6-trifluorostyryl)aniline (4w).** Procedure B was used. Yield 63%. Light yellow crystals from hexane. Mp 127–128 °C.  $^1\text{H}$  NMR:  $\delta$  7.45 (d, 2H,  $J$  = 8.8 Hz), 7.29 (d, 1H,  $J$  = 16.8 Hz), 6.91 (t, 2H,  $J$  = 9.2 Hz,  $J$  = 8.8 Hz), 6.83 (d, 1H,  $J$  = 16.8 Hz), 6.75 (d, 2H,  $J$  = 8.8 Hz), 2.99 (s, 6H).  $^{13}\text{C}$  NMR:  $\delta$  160.87 (dd,  $J$  = 249.1 Hz,  $J$  = 248.9 Hz), 160.72 (dd,  $J$  = 249.0 Hz), 151.09, 135.59 (t,  $J$  = 7.7 Hz,  $J$  = 8.3 Hz), 127.94, 125.24, 112.38, 108.80, 100.65 (dd,  $J$  = 25.8 Hz), 39.64. MS:  $m/z$  (%) 277 (100), 276 (75), 261 (29). Anal. Calcd for  $\text{C}_{16}\text{H}_{14}\text{F}_3\text{N}$ : C, 69.30; H, 5.09. Found: C, 69.49; H, 4.99.

**4-(2,6-Difluorophenethyl)-*N,N*-dimethylaniline (5r).** To 150 mg (0.58 mmol) of **4r** in 10 mL of THF was added 50 mg of 10% Pd–C. The mixture was hydrogenated at 40 psi on a Parr shaker for 5 h. The mixture was filtered through Celite and chromatographed using 1:10 EtOAc/hexane to afford 110 mg (76%) of **5r**: colorless crystals from hexane. Mp 42–43 °C.  $^1\text{H}$  NMR:  $\delta$  7.31–7.23 (m, 1H), 7.02 (d, 2H,  $J$  = 8.4 Hz), 6.94 (t, 2H,  $J$  = 8.4 Hz,  $J$  = 8.0 Hz), 6.66 (d, 2H,  $J$  = 8.4 Hz), 2.90–2.89 (m, 2H), 2.85 (s, 6H), 2.77–2.73 (m, 2H).  $^{13}\text{C}$  NMR:  $\delta$  161.72 (d,  $J$  = 243.7 Hz),

161.63 (d,  $J = 244.5$  Hz), 149.62, 128.98, 128.94, 128.15 (t,  $J = 9.8$  Hz,  $J = 10.7$  Hz), 117.36 (t,  $J = 20.5$  Hz), 112.88, 111.25 (d,  $J = 19.8$  Hz), 111.18 (d,  $J = 19.0$  Hz), 40.10, 34.73, 24.75. MS:  $m/z$  (%) 261 (40), 134 (100), 118 (27), 91 (22). Anal. Calcd for  $C_{16}H_{17}F_2N$ : C, 73.54; H, 6.56. Found: C, 73.53; H, 6.49.

**Cell Culture and Transfection.** HEK293T, HCT116, and SW480 cells were grown in DMEM medium (Mediatech) supplemented with 10% fetal bovine serum and 1% penicillin/streptomycin. LS174T cells were grown in RPMI medium (Mediatech) supplemented with 5% fetal bovine serum and 1% penicillin/streptomycin. HEK293T cells were transiently transfected using the calcium phosphate method as described previously.<sup>37</sup>

**Western Blot.** Western blot was performed as described previously.<sup>37</sup> The following antibodies were used:  $\beta$ -catenin (Sigma, no. C2206), c-Myc (Epitomics, no. 1472-1), Axin2 (Cell Signaling, no. 2151),  $\beta$ -actin (Sigma, no. A1978), TCF4 (Epitomics, no. 2114-1), pygopus2 (Santa Cruz, no. sc-74878), and cyclin D1 (Cell Signaling, no. 2926).

**RT-PCR.** LS174 cells were treated with DMSO or Wnt inhibitors. After 36 h, RNA was isolated using the RNeasy kit (Qiagen). RT-PCR was performed as described previously.<sup>37</sup> The following primers were used.  $\beta$ -Actin: 5'-CAACCGCGAGAAGATGAC-3', 5'-AGGAAGGCT-GGAAGAGTG-3'. Survivin: 5'-CATTCGTCCGGTTGCGCTTTCC-3', 5'-GCGCACTTTCTCCGAGTTTCC-3'. c-Myc: 5'-TGGGCT-GTGAGGAGTTTG-3', 5'-TATGTGGAGCGGCTTCTCG-3'. Axin2: 5'-CACCACCACCACCATTTC-3', 5'-GCATCCACTGCCAGACATCC-3'. TCF4: 5'-CACCACATCATACTACAC-3', 5'-CGACCTTTGCTCTCATTTC-3'. Pygopus2: 5'-GGCCGGTCTGCAAA-TGAAG-3', 5'-TCCACCTCCAGTGCTGTAG-3'. Lgr5: 5'-CCTGC-TTGACTTTGAGGAAGAC-3', 5'-ATGTTCACTGCTGCGATGAC-3'. CD44: 5'-CAGAATGGCTGATCATCTTG-3', 5'-CAAATGCACCA-TTCTCTGAG-3'. Ki67: 5'-ACAGAGTGCTCAACAACCTTC-3', 5'-GTTGCGAGCATTATCAG-3'.

**Luciferase and Cell Proliferation Assays.** HEK293T cells were transiently transfected in a 12-well plate with 0.2  $\mu$ g of the Super8xTOPFlash reporter and 0.05  $\mu$ g of Renilla luciferase reporter. Culture medium was changed after 12 h. After 6 h, cells were treated with DMSO or Wnt inhibitors for 12 h and then treated with 25 mM LiCl or Wnt conditioned medium. After 12 h, cells were harvested and luciferase activity was measured by a dual-luciferase reporter assay system (Promega, Madison WI). All conditions were done in triplicate, and each experiment was carried out at least two times. For cell proliferation assay, CRC cells were treated with DMSO or inhibitors for 2 and 4 days. The cell numbers and viability were analyzed by Vi-Cell cell viability analyzer.

**In Vivo Studies.** LS174 cells ( $2 \times 10^6$ ) were injected subcutaneously into both flanks of 6–8 week C57BL/6J athymic nude mice as previously described.<sup>37</sup> **4r** was dissolved in corn oil. The mice were treated with 20 (mg/kg)/day of **4r** by ip injection (50  $\mu$ L/mouse). Control mice were treated with the same volume of corn oil. The body weight and tumor growth were analyzed twice weekly for 1 month. Tumor size was measured using a digital caliper. The tumor volume was calculated by the formula  $V = \frac{1}{2}LW^2$  (mm<sup>3</sup>).

**Immunofluorescence.** Cells grown on cover glass were fixed by 4% paraformaldehyde for 20 min at room temperature. The cells were permeabilized with PBS containing 0.3% (w/v) Triton X-100 and blocked by 5% normal goat serum in PBS for 30 min. Anti- $\beta$ -catenin antibody (1:300, Sigma, St. Louis, MO) was diluted in blocking solution and incubated with cells overnight. The cells were washed 3 times with PBS and further incubated with Alexa-488-labeled anti-rabbit IgG (1:500) diluted in PBS for 40 min. The cover glasses were washed, mounted on glass slides, viewed and photographed with an Olympus FW1000 confocal microscope.

Cells grown on cover glass were treated with fluorescent compounds for 2, 6, 12, and 24 h. Treated cells were fixed by 4% paraformaldehyde

for 20 min at room temperature. Then cells were washed 3 times with PBS and mounted on glass slides, viewed under the fluorescence of 405 nm wavelength, and photographed with an Olympus FW1000 confocal microscope.

## ■ ASSOCIATED CONTENT

**S Supporting Information.** <sup>1</sup>H and <sup>13</sup>C NMR spectra for the compounds described in this paper. This material is available free of charge via the Internet at <http://pubs.acs.org>.

## ■ AUTHOR INFORMATION

### Corresponding Author

\*Phone: 859-323-4558. Fax: 859-257-6030. E-mail: [chunming.liu@uky.edu](mailto:chunming.liu@uky.edu).

## ■ ACKNOWLEDGMENT

We thank Center for Clinical and Translational Science at University of Kentucky for CCTS Pilot Award. C.L. was supported by Grant R01 DK071976 from the NIH. B.M.E. was supported by UK SPORE Grant P20 CA 150343. D.S.W. was supported by the Office of the Vice President for Research, and the Organic Synthesis Core Facility was supported by NIH Grant 2P20 RR020171 from the National Center for Research Resources.

## ■ ABBREVIATIONS USED

CRC, colorectal cancer; APC, adenomatous polyposis coli; resveratrol, *trans*-resveratrol or (*E*)-3,5,4'-trihydroxystilbene; **4r**, (*E*)-4-(2,6-difluorostyryl)-*N,N*-dimethylaniline

## ■ REFERENCES

- (1) Clevers, H. Wnt/ $\beta$ -catenin signaling in development and disease. *Cell* **2006**, *127*, 469–480.
- (2) van Amerongen, R.; Nusse, R. Towards an integrated view of Wnt signaling in development. *Development* **2009**, *136*, 3205–3214.
- (3) Giles, R. H.; van Es, J. H.; Clevers, H. Caught up in a Wnt storm: Wnt signaling in cancer. *Biochim. Biophys. Acta* **2003**, *1653*, 1–24.
- (4) Kinzler, K. W.; Vogelstein, B. Lessons from hereditary colorectal cancer. *Cell* **1996**, *87*, 159–170.
- (5) Polakis, P. Wnt signaling and cancer. *Genes Dev.* **2000**, *14*, 1837–1851.
- (6) Liu, C.; Kato, Y.; Zhang, Z.; Do, V. M.; Yankner, B. A.; He, X.  $\beta$ -Trcp couples  $\beta$ -catenin phosphorylation-degradation and regulates Xenopus axis formation. *Proc. Natl. Acad. Sci. U.S.A.* **1999**, *96*, 6273–6278.
- (7) Liu, C.; Li, Y.; Semenov, M.; Han, C.; Baeg, G. H.; Tan, Y.; Zhang, Z.; Lin, X.; He, X. Control of  $\beta$ -catenin phosphorylation/degradation by a dual-kinase mechanism. *Cell* **2002**, *108*, 837–847.
- (8) Zeng, X.; Tamai, K.; Doble, B.; Li, S.; Huang, H.; Habas, R.; Okamura, H.; Woodgett, J.; He, X. A dual-kinase mechanism for Wnt coreceptor phosphorylation and activation. *Nature* **2005**, *438*, 873–877.
- (9) Zeng, X.; Huang, H.; Tamai, K.; Zhang, X.; Harada, Y.; Yokota, C.; Almeida, K.; Wang, J.; Doble, B.; Woodgett, J.; Wynshaw-Boris, A.; Hsieh, J. C.; He, X. Initiation of Wnt signaling: control of Wnt coreceptor Lrp6 phosphorylation/activation via frizzled, dishevelled and axin functions. *Development* **2008**, *135*, 367–375.
- (10) Yang, J.; Zhang, W.; Evans, P. M.; Chen, X.; He, X.; Liu, C. Adenomatous polyposis coli (APC) differentially regulates  $\beta$ -catenin phosphorylation and ubiquitination in colon cancer cells. *J. Biol. Chem.* **2006**, *281*, 17751–17757.

- (11) Huang, S. M.; Mishina, Y. M.; Liu, S.; Cheung, A.; Stegmeier, F.; Michaud, G. A.; Charlat, O.; Willellette, E.; Zhang, Y.; Wiessner, S.; Hild, M.; Shi, X.; Wilson, C. J.; Mickanin, C.; Myer, V.; Fazal, A.; Tomlinson, R.; Serluca, F.; Shao, W.; Cheng, H.; Shultz, M.; Rau, C.; Schirle, M.; Schlegl, J.; Ghidelli, S.; Fawell, S.; Lu, C.; Curtis, D.; Kirschner, M. W.; Lengauer, C.; Finan, P. M.; Tallarico, J. A.; Bouwmeester, T.; Porter, J. A.; Bauer, A.; Cong, F. Tankyrase inhibition stabilizes axin and antagonizes Wnt signalling. *Nature* **2009**, *461*, 614–620.
- (12) Chen, B.; Dodge, M. E.; Tang, W.; Lu, J.; Ma, Z.; Fan, C. W.; Wei, S.; Hao, W.; Kilgore, J.; Williams, N. S.; Roth, M. G.; Amatruda, J. F.; Chen, C.; Lum, L. Small molecule-mediated disruption of Wnt-dependent signaling in tissue regeneration and cancer. *Nat. Chem. Biol.* **2009**, *5*, 100–107.
- (13) Liu, C.; He, X. Destruction of a destructor: a new avenue for cancer therapeutics targeting the Wnt pathway. *J. Mol. Cell Biol.* **2010**, *2*, 70–73.
- (14) Barker, N.; Clevers, H. Mining the Wnt pathway for cancer therapeutics. *Nat. Rev. Drug Discovery* **2006**, *5*, 997–1014.
- (15) Garber, K. Drugging the Wnt pathway: problems and progress. *J. Natl. Cancer Inst.* **2009**, *101*, 548–550.
- (16) Signorelli, P.; Ghidoni, R. Resveratrol as an anticancer nutrient: molecular basis, open questions and promises. *J. Nutr. Biochem.* **2005**, *16*, 449–466.
- (17) Athar, M.; Back, J. H.; Tang, X.; Kim, K. H.; Kopelovich, L.; Bickers, D. R.; Kim, A. L. Resveratrol: a review of preclinical studies for human cancer prevention. *Toxicol. Appl. Pharmacol.* **2007**, *224*, 274–283.
- (18) Suh, N.; Paul, S.; Hao, X.; Simi, B.; Xiao, H.; Rimando, A. M.; Reddy, B. S. Pterostilbene, an active constituent of blueberries, suppresses aberrant crypt foci formation in the azoxymethane-induced colon carcinogenesis model in rats. *Clin. Cancer Res.* **2007**, *13*, 350–355.
- (19) Vanamala, J.; Reddivari, L.; Radhakrishnan, S.; Tarver, C. Resveratrol suppresses IGF-1 induced human colon cancer cell proliferation and elevates apoptosis via suppression of IGF-1R/Wnt and activation of p53 signaling pathways. *BMC Cancer* **2010**, *10*, 238.
- (20) Roccaro, A. M.; Leleu, X.; Sacco, A.; Moreau, A. S.; Hatjiharissi, E.; Jia, X.; Xu, L.; Ciccarelli, B.; Patterson, C. J.; Ngo, H. T.; Russo, D.; Vacca, A.; Dammacco, F.; Anderson, K. C.; Ghobrial, I. M.; Treon, S. P. Resveratrol exerts antiproliferative activity and induces apoptosis in Waldenstrom's macroglobulinemia. *Clin. Cancer Res.* **2008**, *14*, 1849–1858.
- (21) Hope, C.; Planutis, K.; Planutiene, M.; Moyer, M. P.; Johal, K. S.; Woo, J.; Santoso, C.; Hanson, J. A.; Holcombe, R. F. Low concentrations of resveratrol inhibit Wnt signal throughput in colon-derived cells: implications for colon cancer prevention. *Mol. Nutr. Food Res.* **2008**, *52* (Suppl. 1), S52–S61.
- (22) Pecere, T.; Gazzola, M. V.; Mucignat, C.; Parolin, C.; Vecchia, F. D.; Cavaggioni, A.; Basso, G.; Diaspro, A.; Salvato, B.; Carli, M.; Palu, G. Aloe-emodin is a new type of anticancer agent with selective activity against neuroectodermal tumors. *Cancer Res.* **2000**, *60*, 2800–2804.
- (23) Chiang, Y. J.; Hsiao, S. J.; Yver, D.; Cushman, S. W.; Tessarollo, L.; Smith, S.; Hodes, R. J. Tankyrase 1 and tankyrase 2 are essential but redundant for mouse embryonic development. *PLoS One* **2008**, *3*, e2639.
- (24) Choi, H. Y.; Lim, J. E.; Hong, J. H. Curcumin interrupts the interaction between the androgen receptor and Wnt/beta-catenin signaling pathway in LNCaP prostate cancer cells. *Prostate Cancer Prostatic Dis.* **2010**, *13*, 343–349.
- (25) Kim, J.; Zhang, X.; Rieger-Christ, K. M.; Summerhayes, I. C.; Wazer, D. E.; Paulson, K. E.; Yee, A. S. Suppression of Wnt signaling by the green tea compound (–)-epigallocatechin 3-gallate (EGCG) in invasive breast cancer cells. Requirement of the transcriptional repressor HBP1. *J. Biol. Chem.* **2006**, *281*, 10865–10875.
- (26) Leow, P. C.; Tian, Q.; Ong, Z. Y.; Yang, Z.; Ee, P. L. Antitumor activity of natural compounds, curcumin and PKF118-310, as Wnt/beta-catenin antagonists against human osteosarcoma cells. *Invest. New Drugs* **2010**, *28*, 766–782.
- (27) Paul, S.; DeCastro, A. J.; Lee, H. J.; Smolarek, A. K.; So, J. Y.; Simi, B.; Wang, C. X.; Zhou, R.; Rimando, A. M.; Suh, N. Dietary intake of pterostilbene, a constituent of blueberries, inhibits the beta-catenin/p65 downstream signaling pathway and colon carcinogenesis in rats. *Carcinogenesis* **2010**, *31*, 1272–1278.
- (28) Zhou, H.; Shang, L.; Li, X.; Zhang, X.; Gao, G.; Guo, C.; Chen, B.; Liu, Q.; Gong, Y.; Shao, C. Resveratrol augments the canonical Wnt signaling pathway in promoting osteoblastic differentiation of multipotent mesenchymal cells. *Exp. Cell Res.* **2009**, *315*, 2953–2962.
- (29) Wang, H.; Zhou, H.; Zou, Y.; Liu, Q.; Guo, C.; Gao, G.; Shao, C.; Gong, Y. Resveratrol modulates angiogenesis through the GSK3beta/beta-catenin/TCF-dependent pathway in human endothelial cells. *Biochem. Pharmacol.* **2010**, *80*, 1386–1395.
- (30) Barker, N.; van Es, J. H.; Kuipers, J.; Kujala, P.; van den Born, M.; Cozijnsen, M.; Haegebarth, A.; Korving, J.; Begthel, H.; Peters, P. J.; Clevers, H. Identification of stem cells in small intestine and colon by marker gene Lgr5. *Nature* **2007**, *449*, 1003–1007.
- (31) Henry, C.; Vitrac, X.; Decendit, A.; Ennamany, R.; Krisa, S.; Merillon, J. M. Cellular uptake and efflux of trans-piceid and its aglycone trans-resveratrol on the apical membrane of human intestinal Caco-2 cells. *J. Agric. Food Chem.* **2005**, *53*, 798–803.
- (32) Gu, B.; Watanabe, K.; Dai, X. Epithelial stem cells: an epigenetic and Wnt-centric perspective. *J. Cell. Biochem.* **2010**, *110*, 1279–1287.
- (33) Saegusa, M.; Hashimura, M.; Kuwata, T.; Hamano, M.; Okayasu, I. Upregulation of TCF4 expression as a transcriptional target of beta-catenin/p300 complexes during trans-differentiation of endometrial carcinoma cells. *Lab. Invest.* **2005**, *85*, 768–779.
- (34) Narender, T.; Papi Reddy, K.; Madhur, G. Synthesis of (E)-stilbenes and (E,E)-1,4-diphenylbuta-1,3-diene promoted by boron trifluoride–diethyl ether complex. *Synthesis* **2009**, *22*, 3791–3796.
- (35) Gester, S.; Pietzsch, J.; Wuest, F. R. Synthesis of <sup>18</sup>F-labelled stilbenes from 4-(<sup>18</sup>F)-fluorobenzaldehyde using the Horner–Wadsworth–Emmons reaction. *J. Labelled Compd. Radiopharm.* **2007**, *50*, 105–113.
- (36) Moran, B. W.; Anderson, F. P.; Devery, A.; Cloonan, S.; Butler, W. E.; Varughese, S.; Draper, S. M.; Kenny, P. T. Synthesis, structural characterisation and biological evaluation of fluorinated analogues of resveratrol. *Bioorg. Med. Chem.* **2009**, *17*, 4510–4522.
- (37) Zhang, W.; Chen, X.; Kato, Y.; Evans, P. M.; Yuan, S.; Yang, J.; Rychahou, P. G.; Yang, V. W.; He, X.; Evers, B. M.; Liu, C. Novel cross talk of Kruppel-like factor 4 and beta-catenin regulates normal intestinal homeostasis and tumor repression. *Mol. Cell. Biol.* **2006**, *26*, 2055–2064.